

PAPER • OPEN ACCESS

Radiation interaction properties of various polymers, saturated and unsaturated fatty acids: A comparative investigation of Monte carlo simulation and NISTXCOM

To cite this article: Varsha A. Bhalerao et al/2020 *J. Phys.: Conf. Ser.* 1644 012024

View the [article online](#) for updates and enhancements.



IOP ebooks™

Bringing together innovative digital publishing with leading authors from the global scientific community.

Start exploring the collection—download the first chapter of every title for free.

Radiation interaction properties of various polymers, saturated and unsaturated fatty acids: A comparative investigation of Monte carlo simulation and NISTXCOM

Varsha A. Bhalerao¹, Rajkumar M. Lokhande², Shrikant B. Bhosale³, Pankaj P. Khirade⁴, Sandip V. Mahajan³, D. K. Gaikwad⁵, Ashok M. Chavan¹

¹Department of Botany, Dr. Babasaheb Ambedkar Marathwada University, Aurangabad, India

²Department of Physics, Shirish Madhukarrao Chaudhari College, Jalgaon (MS), 425001, India

³Department of Botany, S. M. Dnyandeo Mohekar College, Kalamb, Osmanabad (MS), 413606 India

⁴Department of Physics, Shri Shivaji Science College, Amravati (MS), 444603, Maharashtra, India

⁵Department of Physics, ACS College, Dharangaon, 425105 India

rajml358@gmail.com

Abstract. This work represents the study of mass attenuation coefficient, total atomic cross section, total electronic cross section, effective atomic number, effective electron density and half value layer for selected three polymers : Polyacetylene (C_2H_2n), Polyethylene (C_2H_4n), Polypyrrole (C_4H_5n) seven Saturated fatty Acids : Arachidic Acids ($C_{20}H_{32}O_2$), Capric Acid ($C_{10}H_{20}O_2$), Caprylic Acid ($C_8H_{16}O_2$), Cerotic Acid ($C_{26}H_{52}O_2$), Lauric Acid ($C_{12}H_{24}O_2$), Myristic Acid ($C_{14}H_{28}O_2$), Palmitic Acid ($C_{16}H_{32}O_2$) and Six Unsaturated fatty Acids : Arachidonic Acid ($C_{20}H_{32}O_2$), Decosahexaenoic Acid ($C_{22}H_{32}O_2$), Elaidic Acid ($C_{18}H_{34}O_2$), Linoleic Acid ($C_{18}H_{32}O_2$), Erucic Acid ($C_{22}H_{42}O_2$), Oleic Acid ($C_{18}H_{34}O_2$) using NIST-XCOM and Geant4 Monte-Carlo simulation at the energy range 122 keV to 1330keV. Successfully designed narrow beam geometry in Geant4 code for low energy electromagnetic interaction study. We found the errors within 0.001% in the determined results of mass attenuation coefficient and showed Geant4 is a powerful toolkit for measurement of radiation interaction parameter with matter. The variation in effective atomic number and effective electron density with incident photon energy were observed due to the prevalence of photon interaction processes. The Monte-Carlo simulations and theoretical simulation results have been showed that the polymers have good shielding properties as compared with saturated and unsaturated fatty acids. From obtained results, it was noticed that Geant4 Monte-Carlo is in good accord XCOM database.



Content from this work may be used under the terms of the Creative Commons Attribution 3.0 licence. Any further distribution of this work must maintain attribution to the author(s) and the title of the work, journal citation and DOI.

Published under licence by IOP Publishing Ltd

1. Introduction

In the last two decades, 1.4 crore new cancer cases were noted in the world and more than 3 crore people living with cancer disease reported by International Agency for Research on Cancer (IARC-WHO)^{1,2}. The ionising radiation interaction with biomaterial provides valuable data for preclinical radiotherapy applications. The amino acid, carbohydrate, protein, fatty acids and oils are the building blocks of living cells and perform variety of physiological functions³. The advances in radiation biology introduced the innovation of radiation interaction study of biomaterial such as fatty acids, amino acid, carbohydrates and other materials provides significant applications in radiation dosimetry, medical physics, agriculture, industries, radiation diagnosis, drug delivery and shielding purpose⁴⁻¹². The fatty acids used for the detection of cancerous tumour for biochemical and epidemiological to development of tumours and the unsaturated fatty acids detect the limit of cancerous tumours in vitro and vivo^{13,14}. Since few decades, the polymers have also been used for drug delivery for high therapeutic concentration of chemotherapy for applying treatment to the cancer patients¹⁵. The mass attenuation coefficient (μ_m), total atomic cross section, total electronic cross section, effective atomic number (Z_{eff}), effective electron density (N_{eff}), and half value layer are fundamental parameter to finding the penetration and energy deposition of x-ray and gamma radiation⁽¹⁶⁾. Monte-Carlo simulation is found to be most effective tool to determine radiation interaction parameters in diverse kinds of tissue equivalent biomaterial and composites for fundamental ionizing radiation parameter and shielding properties¹⁷⁻¹⁹. There are many Monte-Carlo simulation codes are available for the study of radiation transportation, particle physics, medical physics, Cosmo-physics, radiotherapy, radiation biology namely MCNP, GEANT4 and FLUKA²⁰⁻²³. The many author investigations study of radiation interactions with matter with different electromagnetic processes through the Monte Carlo methods such as oil and soil samples, carbohydrates, glass materials, and nanoparticles²⁴⁻²⁷.

The present study focused on the validation of Geant4 Monte Carlo code for electromagnetic interaction process (Compton and Rayleigh scattering, photoelectric absorption, and pair production) with some polymers, saturated and unsaturated fatty acids versus U. S. Government National Institute of Standards and Technology (NIST) XCOM database. Construction of NaI (TI) narrow beam geometry set up was done using Geant4 Monte Carlo method in computer environment. Study the shielding properties especially selected biomaterials polymers, saturated and unsaturated fatty acids at the energy region 122 keV to 1330 keV. Here we demonstrate the biomaterial (polymers, saturated and unsaturated fatty acids) having fundamental shielding properties with corresponding ionising radiation parameter Z_{eff} , N_{eff} and HVL. Comparing results between XCOM and Geant4 Monte Carlo method verifying with the statistical tool t test for significant role.

2. Materials and Methods

In the present study, we determined the mass attenuation coefficient, total atomic cross section, total electronic cross section, effective atomic number, effective electron density and half value layer for selected three polymers such as Polyacetylene (C_2H_2n), Polyethylene (C_2H_4n), Polypyrrole (C_4H_5n) and seven Saturated fatty Acids such as Arachidic Acids ($C_{20}H_{32}O_2$), Capric Acid ($C_{10}H_{20}O_2$), Caprylic Acid ($C_8H_{16}O_2$), Cerotic Acid ($C_{26}H_{52}O_2$), Lauric Acid ($C_{12}H_{24}O_2$), Myristic Acid ($C_{14}H_{28}O_2$), Palmitic Acid ($C_{16}H_{32}O_2$) and Six Unsaturated fatty Acids : Arachidonic Acid ($C_{20}H_{32}O_2$), Docosahexaenic Acid ($C_{22}H_{32}O_2$), Eliadic Acid ($C_{18}H_{34}O_2$), Lenoleic Acid ($C_{18}H_{32}O_2$), Erucic Acid ($C_{22}H_{42}O_2$) and Oleic Acid ($C_{18}H_{34}O_2$) in the energy range 122 to 1330 keV. The XCOM database shows none zero values for all the process at selected energy region there Compton (Coherent and incoherent sections) and pair production (In Nuclear field and In Electron field).

2.1. Geant4

Geant4 Monte Carlo simulation method is an object oriented toolkit depending on C++ programming language, it is used for measurement of radiation interaction with matter at wide energy range 250 eV to 100 TeV²⁸. The study of electromagnetic radiation in the Geant4 environment is available for low EM Test package; we study the EM Test 13, 15 and 18 for low electromagnetic interaction. The

Geant4 method for electromagnetic package was especially applied for narrow beam geometry. The study carried out in the UNIX operating system Geant4 version 9.06.p01 for all gamma sources. We were calculated attenuation coefficient using computer environment and Geant4 applications G4RunManager for low energy physics the observed Electromagnetic Standard G4PhotoElectricEffect, G4ComptonScattering, G4GammaConversion (pair production). We have to know the primary information to construction of detector geometry of electromagnetic package for Geant4 simulation. There are three stages First stage construction, narrow beam geometry set up of monochromatic source expose the radiation selected gamma energy to material and detector and set unique distance between source-sample-detector. Second stage set the energy, here we select the energy region 122, 356, 511, 662, 1170, 1275 and 1330 keV and chemical composition, density, elemental weight fraction and thicknesses of the selected polymers saturated and unsaturated fatty acids, set physical process photoelectric, Compton (Coherent and incoherent) and pair production corresponding to photon energy. Third stage measured simulation value by using GMcalculator after 10^6 times hits of gamma radiation on selected biomaterial at particular thickness.

2.2. NIST XCOM

The XCOM data provided by the National Institute of standards and technology through US government. The XCOM provides X-ray, gamma ray and bremsstrahlung to photon cross section and total attenuation coefficient of element, mixture and compounds at the energy range 1 keV to 100 GeV for the applications of medical radiation physics²⁹. Mass attenuation coefficient is the probability between the incident photon energy ($h\nu$) and sample per mass unit area. Mass attenuation coefficient and mass energy absorption coefficient were described by Hubbell and Seltzer³⁰ for the application of radiotherapy and dosimetric interest.

The theoretical investigation of mass attenuation coefficient is depends on Lambert Beers law a parallel ray of X-ray or Gamma ray photons passing through matter is attenuated due to electromagnetic region (absorption and scattering) Figure 1 described the narrow beam setup and mathematically written as

$$I = I_0 \exp(-\mu_m t) \quad (1)$$

Where, I_0 and I are the Incident and transmitted photon intensities of gamma radiations, μ_m is mass attenuation coefficient of the selected biomaterials and t is the thickness of sample. Then mixture rule applied for compound or mixture of element.

$$\left(\frac{\mu}{\rho}\right) = \sum w_i \left(\frac{\mu}{\rho}\right)_i \quad (2)$$

From above formulation we observed the probability of interaction between X-ray, gamma photon and matter of mass per unit area called mass attenuation coefficient.

2.3. The total atomic and electronic cross section

The total atomic cross section can be written mathematically by the following equation;

$$\sigma_{t,a} = \frac{1}{N_A} + \frac{(\mu_m)}{\sum i w_i / A_i} \quad (3)$$

Where N_A is the Avogadro's number and A_i is the atomic number of i^{th} constituent element of biomaterials. With the help of principle of photon interaction total cross section were written as

$$\sigma_{t,a} = \sigma_{pe} + \sigma_{Coh} + \sigma_{incoh} + \sigma_{pair} + \sigma_{trip} + \sigma_{ph.n}$$

The total electronic cross section is mathematically as,

$$\sigma_{t,el} = \frac{1}{N_A} \sum_i^{i=1} \frac{f_i A_i}{Z_i} (\mu_m)_i \quad (4)$$

Where f_i is the number fraction of atoms in element of i^{th} constituent relative to ferrites and Z_i is the atomic number.

2.4. The effective atomic number (Z_{eff})

The effective atomic number can be estimated using equation;

$$Z_{eff} = \frac{\sigma_{t,at}}{\sigma_{t,el}} \quad (5)$$

2.5. Effective electron density (N_{eff})

$$\text{Some text. } N_{eff} = \left(\frac{N_A}{A_{eff}} \right) \times Z_{eff} \quad (6)$$

Where, A_{eff} is effective atomic mass also acknowledged as the ratio of atomic weight and total number of atoms.

2.6. Half value layer (HVL)

The half value layer is mathematically expressed as;

$$HVL = \frac{\ln 2}{\mu} = \frac{0.696}{\mu} \quad (7)$$

Here, μ is the linear attenuation coefficient. The μ is computed from narrow beam geometry setup of Geant4.

3. Results and discussion

Table 1 shows the chemical composition, chemical formula, density, molar mass of the polymers, saturated and unsaturated fatty acids. In the present theoretical investigations we observed radiation interaction study of biomaterials with the help of Geant4 Monte Carlo method and XCOM web datasheet. The mass attenuation coefficient of selected polymers, saturated and unsaturated fatty acids successfully measured with help of Geant4 Monte Carlo and compared XCOM database for total attenuation cross section for without coherent and with coherent at energy region 122 keV to 1330 keV. Table 2 shows variation of mass attenuation coefficient with selected energy region. It is noticed that the mass attenuation coefficient decreases with increasing photon energy for the all selected biomaterials. The mass attenuation coefficients values determined by using Geant4 Monte Carlo method were slightly lower than XCOM database values at low energy. Fig. 2 shows XCOM and Geant4 mass attenuation coefficient values against photon energy of polymers, saturated and unsaturated fatty. It is clearly seen that the XCOM and Geant4 results are in the excellent accord to each other. It is reflected that we were successfully constructed detector geometry in Geant4 and the comparative results having 0.001 % errors. Also the mass attenuation coefficient result verification with the statistical tool t test for of theoretically XCOM and Geant4 Monte Carlo method. Fig. 3 shows the total atomic cross section of the selected biomaterials. It is clear from Fig. 3 that the total atomic cross section decreases with increasing photon energy. Rajamanickam et al., reported the importance of total atomic cross section of high Z materials in the macroscopic study for the development algorithm for the clinical treatments (it gives preclinical treatment planning)³¹. Similarly we determined electronic cross section depicted in Fig. 4. It is seen from that results of electronic cross section decrease with increasing incident photon energy and graphically. The effective atomic number is important parameter for study the effect of gamma radiation for constituent element or elemental compositions of materials. The effective atomic number varies with photon energy i.e. Z_{eff} decreases with increasing photon energy³². Figs. 5(a) Polymers, (b) saturated fatty acids, (c) Unsaturated fatty acids show that there is no change in Z_{eff} at selected energy region (122 keV to 1330 keV). Fig. 4 (a) shows the Z_{eff} versus incident photon energy of polymers. It is seen that the Polyacetylene have the highest effective atomic number as compared to the Polyethylene and Polypyrrole. Fig. 4 (b) shows the Z_{eff} versus incident photon energy of saturated fatty acids. It is seen that the capric acid having highest and Cerotic acid having lowest Z_{eff} as compared to other saturated fatty acids. Fig. 5(c) shows the Z_{eff} versus incident photon energy of unsaturated fatty acids. It is observed that the Arachidonic acid possesses highest and Erucic acid have lowest Z_{eff} as compared to other saturated fatty acids. The graphically representation of effective electron density of the materials shown in Fig. 6(a) Polymers, (b) saturated fatty acids, (c) Unsaturated fatty acids. It is seen that there is no variation with energy as

particular selected energy region. The number of electron density obeys the 10^{23} shows with Eq. 6 is dependent on the effective atomic number. The result reflects there is no change in N_{eff} and Z_{eff} indicates photon absorbed by the material persist longer time due to the elastic scattering where the electron at selected energy region recoiled. The half value layer study investigation under present study for the shielding purpose of the biomaterials and polymers. Earlier many authors suggested that the shielding properties of polymers, one of the authors reported the shielding properties of polymer nanocomposite for the purpose of radiotherapy for decreasing unexpected dose to living tissue¹³. We determined the half value layer using Geant4 Monte Carlo method for narrow beam geometry set up with monochromatic sources at selected energy region 122 keV to 1330 keV. The HVL represent graphically in the Fig. 7. It is observed that HVL increases with increasing incident photon energy. It is also noticed that the HVL values of polymers vary drastically with photon energy as compared to the saturated and unsaturated fatty acids.

Table 1 Chemical composition of all selected polymers, saturated and unsaturated fatty acids

Sr. No.	Materials	Chemical Formula	Molar mass	Density (g/cm ³)
1	Polyacetylene	C ₂ H _{2n}	40.04	0.400
2	Polyethylene	C ₂ H _{4n}	42.06	0.960
3	Polypyrrole	C ₄ H _{5n}	67.09	1.050
4	Arachidic Acid	C ₂₀ H ₃₂ O ₂	304.46	0.922
5	Capric Acid	C ₁₀ H ₂₀ O ₂	172.26	0.893
6	Caprylic Acid	C ₈ H ₁₆ O ₂	144.21	0.910
7	Cerotic Acid	C ₂₆ H ₅₂ O ₂	396.69	0.820
8	Lauric Acid	C ₁₂ H ₂₄ O ₂	200.31	0.880
9	Myristic Acid	C ₁₄ H ₂₈ O ₂	228.37	0.862
10	Palmitic Acid	C ₁₆ H ₃₂ O ₂	356.43	0.853
11	Arachidonic Acid	C ₂₀ H ₃₂ O ₂	304.46	0.922
12	Docosahexaenoic Acid	C ₂₂ H ₃₂ O ₂	248.22	0.943
13	Elaidic Acid	C ₁₈ H ₃₄ O ₂	282.46	0.873
14	Erucic Acid	C ₁₈ H ₃₂ O ₂	238.57	0.860
15	Linoleic Acid	C ₂₂ H ₄₂ O ₂	280.44	0.900
16	Oleic Acid	C ₁₈ H ₃₄ O ₂	282.47	0.895

Table 2 Investigations of Mass Attenuation Coefficients of selected materials

Energy (keV)	122		356		511		662		1170		1275		1330	
	XCOM	Geant4	XCOM	Geant4	XCOM	Geant4	XCOM	Geant4	XCOM	Geant4	XCOM	Geant4	XCOM	Geant4
Polyacetylene	0.1514	0.1507	0.1073	0.1072	0.0928	0.0932	0.0830	0.0835	0.0633	0.0636	0.0606	0.0608	0.0593	0.0595
Polyethylene	0.1607	0.1534	0.1138	0.1044	0.0984	0.0907	0.0880	0.0812	0.0672	0.0619	0.0643	0.0592	0.0629	0.0579
Polypyrrole	0.1539	0.1504	0.1090	0.1070	0.0943	0.0930	0.0843	0.0832	0.0643	0.0636	0.0616	0.0606	0.0602	0.0594
Arachidic Acid	0.1580	0.1587	0.1123	0.1123	0.0976	0.0972	0.0874	0.0869	0.0666	0.0663	0.0637	0.0635	0.0623	0.0621
Capric Acid	0.1563	0.1571	0.1111	0.1112	0.0966	0.0962	0.0865	0.0860	0.0659	0.0656	0.0631	0.0628	0.0617	0.0615
Caprylic Acid	0.1556	0.1564	0.1106	0.1107	0.0961	0.0957	0.0861	0.0856	0.0656	0.0653	0.0628	0.0625	0.0614	0.0612
Cerotic Acid	0.1584	0.2710	0.1126	0.1916	0.0979	0.1657	0.0877	0.1481	0.0668	0.1130	0.0639	0.1081	0.0625	0.1058
Lauric Acid	0.1569	0.1576	0.1115	0.1115	0.0969	0.0965	0.0868	0.0863	0.0662	0.0659	0.0633	0.0630	0.0619	0.0617
Myristic Acid	0.1572	0.1580	0.1178	0.1118	0.0971	0.0967	0.0870	0.0865	0.0663	0.0660	0.0634	0.0632	0.0634	0.0618
Palmitic Acid	0.1575	0.1583	0.1120	0.1120	0.0973	0.0969	0.0872	0.0866	0.0664	0.0661	0.0636	0.0633	0.0622	0.0619
Arachidonic Acid	0.1555	0.1547	0.1101	0.1100	0.0952	0.0956	0.0851	0.0857	0.0650	0.0653	0.0622	0.0624	0.0609	0.0611
Docosahexaenoic Acid	0.1559	0.1537	0.1104	0.1093	0.0955	0.0950	0.0854	0.0851	0.0652	0.0648	0.0624	0.0620	0.0610	0.0607
Elaidic Acid	0.1576	0.1569	0.1116	0.1115	0.0965	0.0969	0.0863	0.0869	0.0659	0.0662	0.0630	0.0633	0.0617	0.0619
Erucic Acid	0.1581	0.1574	0.1119	0.1119	0.0969	0.0973	0.0866	0.0871	0.0661	0.0664	0.0632	0.0635	0.0619	0.0621
Linoleic Acid	0.1567	0.1560	0.1110	0.1109	0.0960	0.0964	0.0858	0.0864	0.0655	0.0658	0.0627	0.0630	0.0613	0.0616
Oleic Acid	0.1585	0.1569	0.1122	0.1115	0.0971	0.0969	0.0868	0.0869	0.0662	0.0662	0.0634	0.0633	0.0620	0.0619

Table 3 T-Test results respective to two groups from Geant4 method and XCOM for selected materials

	Variable 1	Variable 2
Mean	0.156766	0.162954
Variance	4.44E-06	0.000837
Observations	16	16
Pearson Correlation	0.256078	
Hypothesized Mean Difference	0	
df	15	
t Stat	-0.86983	
P(T<=t) one-tail	0.19905	
t Critical one-tail	1.75305	
P(T<=t) two-tail	0.3981	
t Critical two-tail	2.13145	

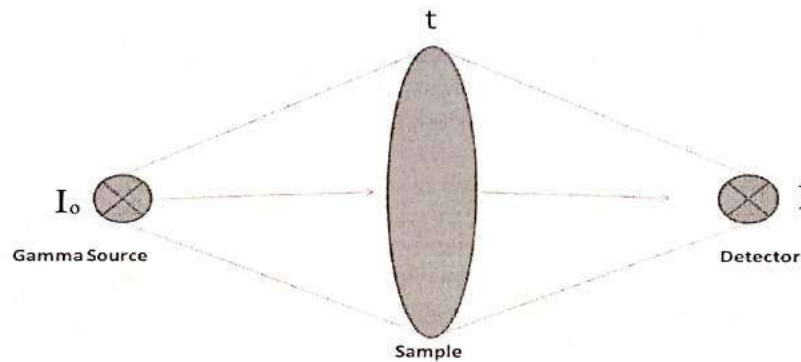


Fig. 1 Schematic View of Narrow Beam Geometry Setup

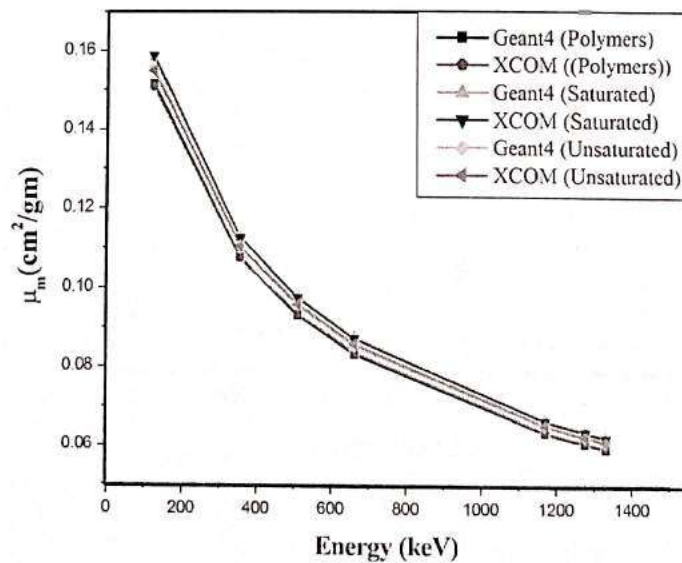


Fig.2 The variation of μ_m Vs incident Photon energy

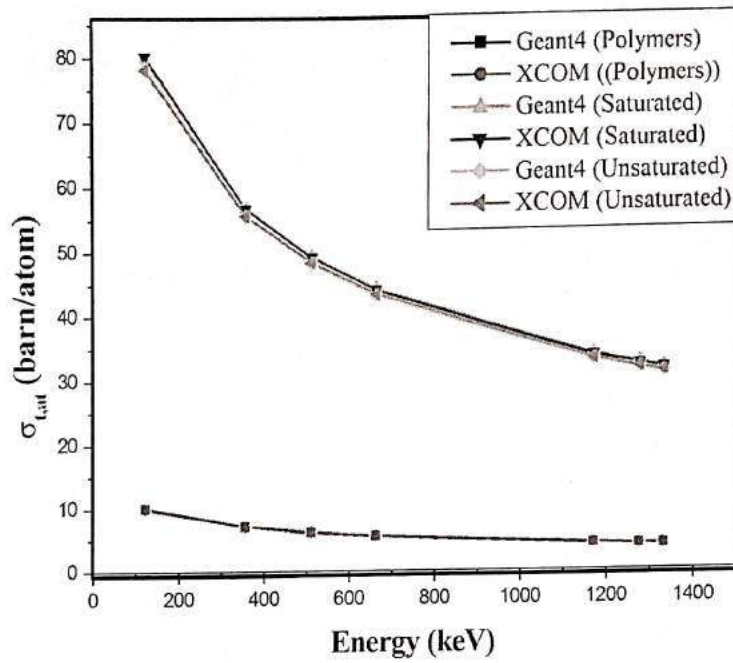


Fig. 3 the Variation $\sigma_{t,at}$ Vs incident Photon energy

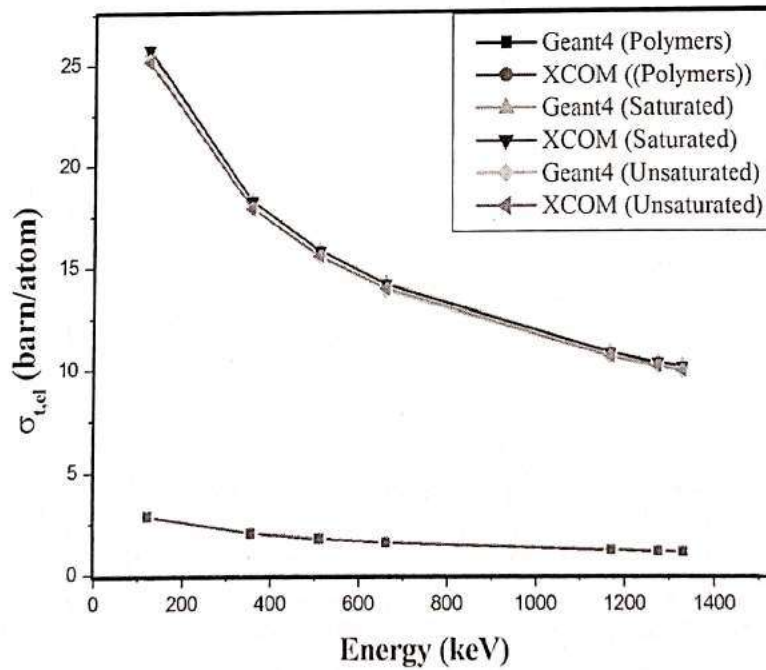


Fig.4 variation of $\sigma_{t,el}$ Vs incident Photon energy

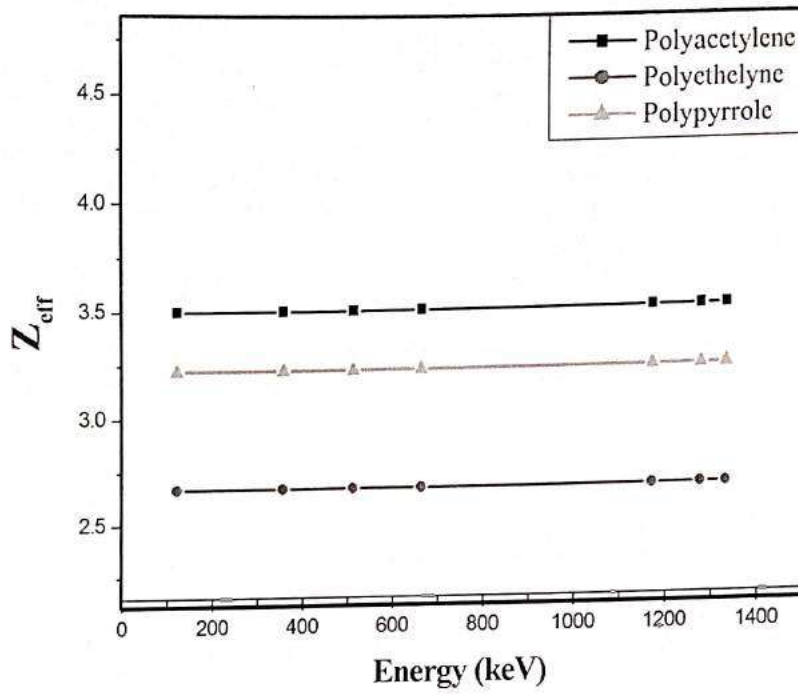


Fig. 5(a) Z_{eff} Vs incident Photon energy

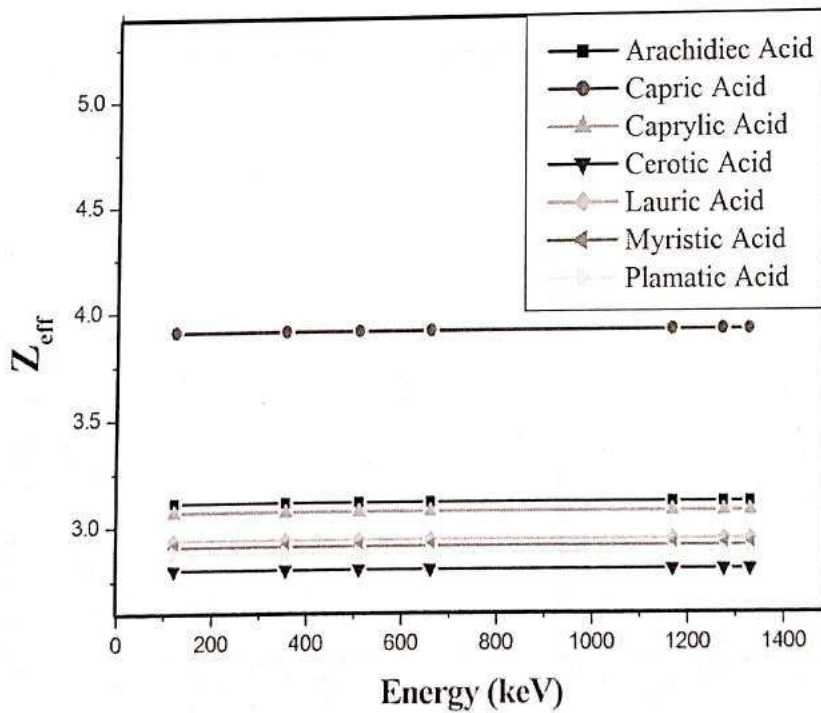


Fig. 5(b) Z_{eff} Vs incident Photon energy

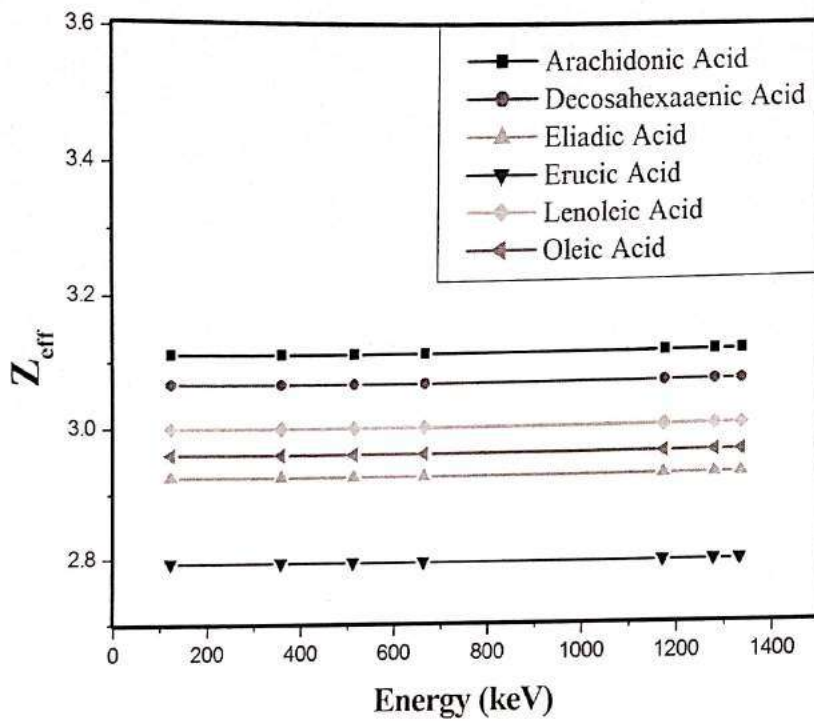


Fig. 5(c) Z_{eff} Vs incident Photon energy

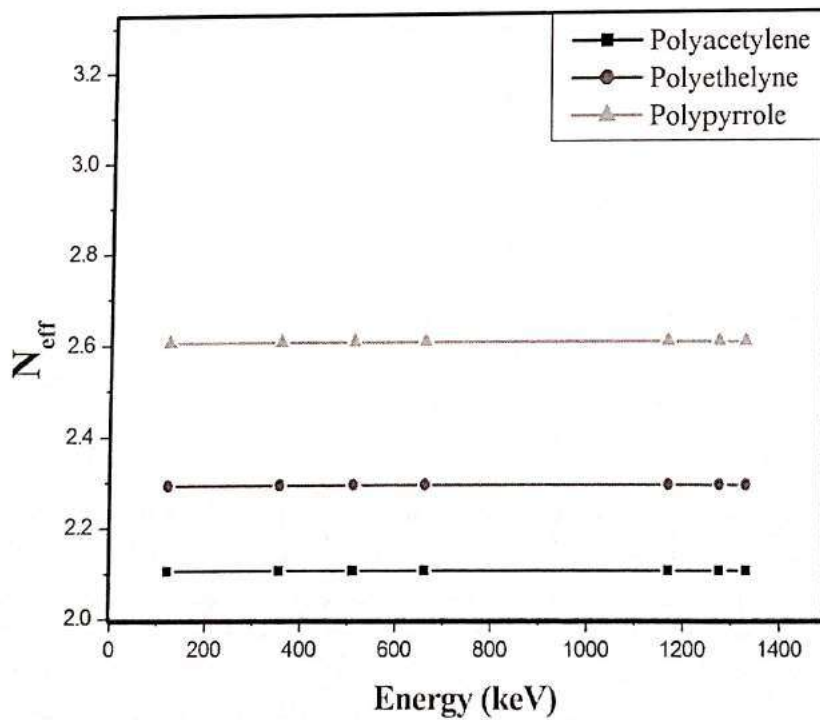


Fig. 6 (a) N_{eff} Vs incident Photon energy

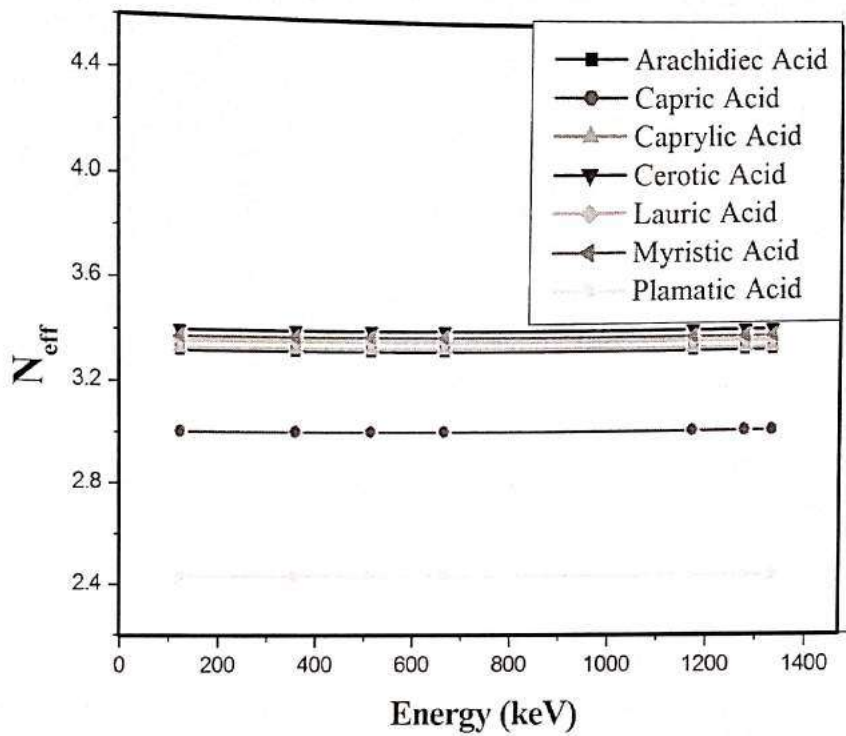


Fig. 6(b) N_{eff} Vs incident Photon energy

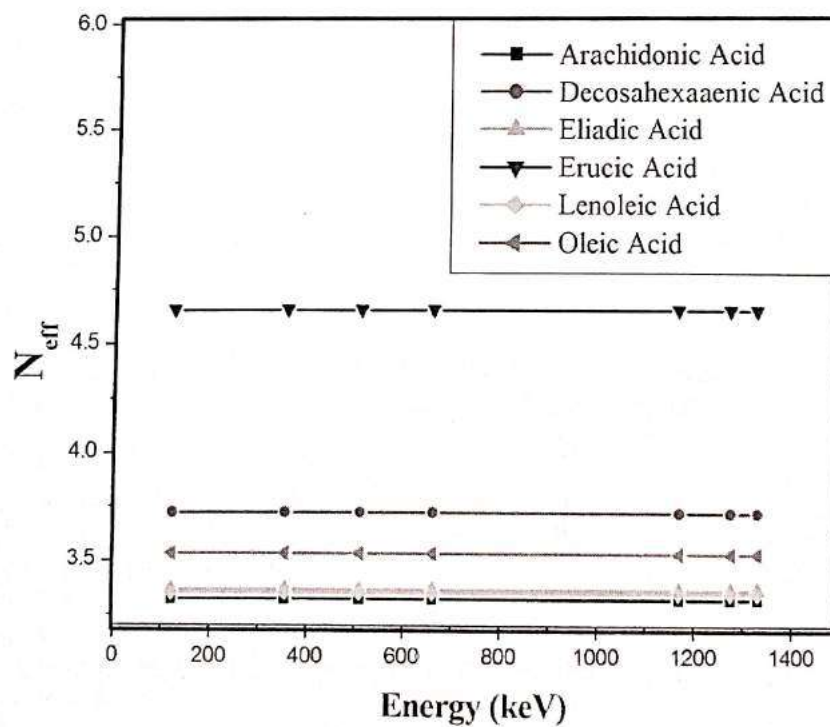


Fig. 6(c) N_{eff} Vs incident Photon energy

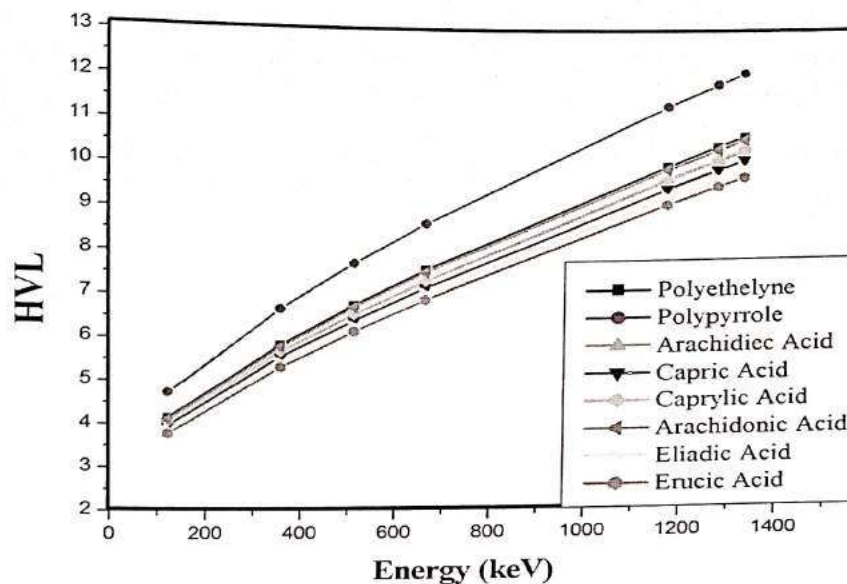


Fig. 7 Variation of HVL Vs incident Photon energy.

4. Conclusions

The Geant4 method and NIST XCOM were used to determine the mass attenuation coefficient, total attenuation coefficient, total electronic cross section, Z_{eff} , N_{eff} and HVL for the selected three polymers, seven saturated and six unsaturated fatty acids at the energy region 122 keV to 1330 keV incident photon energy. The results of the mass attenuation coefficient, total attenuation coefficient, total electronic cross section, Z_{eff} , N_{eff} Values were decreased with the increment of incident photon energy attributed to the Compton scattering photon interaction process. From the results of Z_{eff} and N_{eff} , It is found that polymer has lowest Z_{eff} values than the saturated fatty acid (Capric Acid). The HVL of the selected polymer were observed higher than the fatty acids. Thus it is worth noting that polymers are agonized to radiation damage than fatty acids for the selected energies. The study examine the validation of Geant4 Monte Carlo method compares with XCOM datasheet i.e. both the results having good agreement with each other. Besides, the result obtained from statistical tool T-test of two groups. It is observed that the Geant4 code is powerful toolkit for measuring radiation interaction parameter and applicable for medical physics, radiation biology, dosimetry and radiotherapy.

Acknowledgement

The authors are very much indebted to Santosh B. Phad, Research Scholar, International Institute for Population Sciences (IIPS), Mumbai for their fruitful guidance about statistical tool SPSS T-Test.

References

- [1] Cooke S & Whittington A, *Mater. Sci. eng. C* 60 (2016) 78–83
- [2] "WHO | IARC - International Agency For Research On Cancer". *Who.Int*, 2020, https://www.who.int/ionizing_radiation/research/iarc/en/. Accessed 28 Aug 2020.
- [3] Gaikwad D, Pawar P and Selvam T *Pramana – J. Phys.* 12(2016) 87
- [4] Gounhalli S, Shantappa A, Hanagodimath S. *J App Phys.* 2(4) (2012) 40-48.
- [5] Gaikwad, D. K., Pawar, P. P., & Selvam, T. P., *Radiation Physics and Chemistry*, 138, (2017) 75-80.
- [6] Awasarmol, V. V., Gaikwad, D. K., Raut, S. D., & Pawar, P. P., *Radiation Physics and Chemistry*, 130 (2017) 343-350.

- [7] Obaid, S. S., Sayyed, M. I., Gaikwad, D. K., Tekin, H. O., Elmahroug, Y., & Pawar, P. P., Radiation Effects and Defects in Solids, 173(11-12), (2018)900-914.
- [8] Gowda S, Krishnaveni S, Yashoda T, Umesh T and Gowda R. *Pramana - J Phys.* 63(2004): 529-541.
- [9] Bhosale, R. R., More, C. V., Gaikwad, D. K., Pawar, P. P., & Rode, M. N. Nuclear Technology and Radiation Protection, 32(3), (2017) 288-293.
- [10] Bhosale, R. R., Gaikwad, D. K., Pawar, P. P., & Rode, M. N., Nuclear Technology and Radiation Protection, 31(2), (2016)135-141.
- [11] Bhosale, R. R., Gaikwad, D. K., Pawar, P. P., & Rode, M. N., Radiation Effects and Defects in Solids, 171(5-6), (2016)398-407.
- [12] More C, Lokhande R and Pawar P *Radiat Phys Chem.* 125(2016) 14-20
- [13] Wen B, Deutsch E, Opolon P, Auperin A, Frascogna V, Connault E, and Bourhis J *British Journal of Cancer* (2003) 89, 1102 – 1107
- [14] Antal O, Hackler L, Shen J, Mán I, Hideghéty K, Kitajka K and Puskás L *Lipids in Health and Disease* 2014, 13:142
- [15] Wolinsky J, Colson Y, Grinstaff M, *J. of Controlled Release* 159 (2012) 14–26
- [16] Sayyeda M, Agarb O, Kumar A, Tekind H, Gaikwad D, Obaid S *Chemical Physics* (2019)
- [17] Halil A, *NuclSci Tech* 96(2019) 30:96
- [18] Medhat M and Singh V. *Indian J pure and applied phys.* 54(2016) 137-143.
- [19] Singh VP, Medhat ME, Shirmardi SP, *Radiat Phys Chem.* 106 (2015) 255–260.
- [20] Geant-4 toolkit web site. <http://geant4.fweb.cern.ch/geant4>.
- [21] Amako K, Guatelli S, Ivanchenko V.N., Maire M, Mascialino B, Murakami K, Nieminen P, Pandola L, Parlati S, Pia M.G, Piergentili M, Sasaki T, Urban L., *IEEE T. Nucl. Sci.* 52 (2005)910–918.
- [22] Briesmeister J, MCNP/TPM General Monte Carlo Ne Particle Transport Code Version 4C. RSICC Computer Code Collection, ccc700, Oak Ridge National Laboratory, 2000.
- [23] Ferrari A, Sala P, Fasso A, RanO J (2005) FLUKA: A multi- particle transport code, CERN-2005-010, INFN TC_05/11, SLAC-R-773.
- [24] Stalin, S., Gaikwad, D. K., Samee, M. A., Edukondalu, A., Ahmmad, S. K., Joshi, A. A., & Syed, R. *Ceramics International.* 46 (11), (2020) 17325-1733.
- [25] Lokhande R, Surung B, Pawar P, *Int. J. Adv. Res.* 5(5) (2017) 1733-1740
- [26] Gaikwad, D. K., Sayyed, M. I., Botewad, S. N., Shamsan S, Obaid, Khatari, Z. Y., Gawai, U. P., Feras Afaneh, Shirshat, M. D., and Pawar, P. P., *Journal of Non-Crystalline Solids*, 503, (2019)158-168.
- [27] Sayyed, M., Manjunatha, H. C., Gaikwad, D. K., Obaid, S. S., Zaid, M. H. M., & Matori, K. A., *Digest Journal of Nanomaterials and Biostructures*, 13(3), (2018)701-712.
- [28] Agostinelli S, Allison J, Amako K, Apostolakis J, Araujo H, Arce P, Asai M, Axen D, Banerjee S, Barrand G, Behner F, Bellagamba L, Boudreau J, Broglia L, Brunengo A, Burkhardt H, Chauvie S, Chuma J, Chytrcek R, Cooperman G, Cosmo G, Degtyarenko P, Dell'Acqua A, Depaola G, Dietrich D, Enami R, Feliciello A, Ferguson C, Fesefeldt H, Folger G, Foppiano F, Forti A, Garelli S, Giani S, Giannitrapani R, Gibin D, Gómez Cadenas J, *J. Nucl. Instrum. Methods Phys. Res. A* 2003, 506, 250–303.
- [29] Hubbell J, *Phys. Med. Biol.* 51 (2006) 245-262.
- [30] Berger M, Hubbell J, Seltzer S, Chang J, Coursey J, Sukumar R, Zucker D, Olsen K, XCOM: Photon Cross Sections Database, NIST Standard Reference Database (XGAM), 2010. Available at: <http://www.nist.gov/pml/data/xcom/index.cfm>.
- [31] Rajamanickam T, Muthu S, Murugan P, Pathikonda M, Senthilnathan K, Nambi Raj A, Babu *Asian Pac J Cancer Prev*, 20 (8), 2485-2491
- [32] Lokhande R, More C, Surung B, Pawar P, *Radiation Physics and Chemistry* 141 (2017) 292–299
- [33] Dorel F, *Appl. Sci.* 9 (2019) 3899